SLAC-PUB-112
ITP-168
May, 1965

HIGH-ENERGY γ-RAY SOURCE FROM ELECTRON-POSITRON PAIR ANNIHILATION*

Y. S Tsai

Stanford Linear Accelerator Center
Stanford University, Stanford, California

and

S. M. Swanson and C. K. Iddings

Institute of Theoretical Physics
Stanford University, Stanford, California

(Paper delivered at the International Symposium on Electron and Photon Interactions at High Energies, DESY, June 1965)

*Work supported in part by the U. S. Atomic Energy Commission and in part by the Air Force Office of Scientific Research Grant AF-49(638)-1389.

The purpose of this paper is to continue the investigation of the problems associated with the production of a nearly monochromatic high-energy photon source using the reaction $e^+ + e^- \to 2\gamma$. Some preliminary investigations[1] show that the scheme is very promising for use in conjunction with the bubble chamber and spark chamber types of experiments proposed at the Stanford Linear Accelerator Center. A typical spectrum of γ at a fixed angle is expected to look like Fig. 1. The low energy end of the spectrum shows a typical $1/k$ dependence of the bremsstrahlung from e^+p and e^+e^- collisions. In order to obtain the spectrum, one has to calculate the following four processes in detail:

(a) $e^+ + e^- \to 2\gamma$ and its radiative corrections

(b) $e^+ + e^- \to 3\gamma$

(c) $e^+ + e^- \to e^+ + e^- + \gamma$

(d) $e^+ + p \to e^+ + p + \gamma$

The process (a) and part of the process (b) where the third photon emitted is limited to a low energy [i.e., the effect of the process (b) in the neighborhood of the spike in Fig. 1] were investigated in detail previously.[2]

The processes (b), (c), and (d) constitute the unwelcome background. The hydrogen atom is chosen because the process (d) is proportional to Z^2 (if screening is ignored), whereas the processes (a), (b), and (c) are proportional to Z. The most interesting region of angle θ between the incident positron and outgoing photon is in the neighborhood of $\theta = (2/\gamma)^{\frac{1}{2}}$, where $\gamma = E/m$ and E is the incident positron energy. This results from the following:

1. The ratio of the cross section for process (a) to that of process (d) increases rapidly with angle; therefore, in order to reduce the background

due to (d), the larger the angle the better.

2. The process (c) is symmetric with respect to 90° in the c.m. system of the initial e^+e^- due to symmetry under charge conjugation. $\theta_{c.m.} = 90^\circ$ corresponds to $\theta = (2/\gamma)^{\frac{1}{2}}$ in the laboratory system. For $\theta \ll \gamma^{-\frac{1}{2}}$, (c) and (d) are identical to within a few percent. However, for $\theta > (2/\gamma)^{\frac{1}{2}}$, the process (c) dominates over process (d). Furthermore, the cross section for the process (a) decreases more rapidly than that for process (c) as the angle θ is increased beyond $\theta = (2/\gamma)^{\frac{1}{2}}$. Therefore, no advantage is gained for reduction of background by taking θ much beyond $(2/\gamma)^{\frac{1}{2}}$.

3. The angle θ must not be chosen too large because both the cross section and the energy of the photon in process (a) decrease rapidly with angle. For the three reasons given above we shall concentrate our discussions in the neighborhood of angle $\theta_{c.m.} = 90^\circ$.

The lowest order cross section for process (a) for $1 \gg \theta \gg \gamma^{-1}$ can be written as[2]

$$\frac{d\sigma_{ao}}{d\Omega_k} = \frac{r_o^2}{2} \frac{1}{(1+z)^2} \left(\frac{1}{z} + z \right) , \tag{1}$$

where

$$z = \frac{\gamma\theta^2}{2} . \tag{2}$$

The numerical result is given in column 4 of Table I. The c.m. angle of process (a) is given by

$$\cos \theta_{c.m.} = \frac{1 - z}{1 + z} . \tag{3}$$

The energy of the photon produced by process (a) is

$$\omega_a = E/(1 + z) . \tag{4}$$

The maximum energies of photons produced by processes (b) and (c) are also given by Eq. (4) (in the limit $m/E \to 0$), whereas the corresponding limit for process (d) is given by

$$\omega_{max} = E/[1 + EM^{-1}(1 - \cos\theta)] \tag{5}$$

where M is the mass of the proton. The radiative corrrection δ to process (a) can be written as[2]

$$\frac{d\sigma_a}{d\Omega_k} = \frac{d\sigma_{ao}}{d\Omega_k} (1 + \delta) \tag{6}$$

where

$$\delta \approx -\frac{2\alpha}{\pi} \left\{ \ell n \left(R \frac{\sqrt{z}}{1 + z} \right) - \frac{3}{4} \right\} (\ell n 2\gamma - 1) \tag{7}$$

and $R = \omega_a/\Delta\omega$ (see Fig. 1). Equation (6) represents the area under the curve from A to ω_a as shown in Fig. 1.

For $E = 15$ BeV and $z = 1$ we have[2]

R	δ
200	-0.18
100	-0.15
50	-0.12
25	-0.08
10	-0.04
5	-0.008

For process (d), the energy-angle distribution of the bremsstrahlung is quite adequately given by the Sommerfeld-Schiff formula,[3,4] except that at large angles and large photon energies one has to add minor corrections due to the

proton form factors and kinematics. The Sommerfield-Schiff formula is

$$\left(\frac{d\sigma_d}{d\Omega d\omega}\right)_{\text{Schiff}} = \frac{2\alpha r_o^2}{\pi\omega}\gamma^2\left[\frac{16\ell(1-y)}{(1+\ell)^4} - \frac{(2-y)^2}{(1+\ell)^2}\right.$$
$$\left. + \left[\frac{2-2y+y^2}{(1+\ell)^2} - \frac{4\ell(1-y)}{(1+\ell)^4}\right] 2\ell n[2\gamma(y^{-1}-1)]\right] \tag{8}$$

where $\ell \equiv \gamma^2\theta^2$ and $y = \omega/E$. When $\theta \sim \gamma^{-\frac{1}{2}}$, we have $\ell \gg 1$ and the above formula can be considerably simplified. A numerical example of the behavior of this formula is given in column 5 of Table I. In column 6 we give the result obtained by numerically integrating the exact matrix element[5] for process (d) with the effects of form factors, magnetic moment, and recoil of the proton included. As is to be expected, the difference between the two results is noticeable only for large angles and large γ energies. In general, due to the functional behavior of the integrand, the numerical integration is less reliable at small θ and small ω because of the round-off errors, whereas for large θ and ω the integrand is less singular and the results are reliable to within 1%. Thus columns 5 and 6 are complimentary to each other; namely, for small θ and ω the results of column 5 must be used and for other cases the results of column 6 must be used. The starred quantities in Table I denote the less reliable values.

For the process (c), some heroic efforts were required to obtain the necessary cross section. It is convenient to discuss this process in the c.m. system of the incident $e^+ - e^-$. In the c.m. the cross section must be symmetric with respect to 90° because of symmetry under charge conjugation. There are "8" diagrams contributing to this process. For small $\theta_{c.m.}$, the two diagrams shown in Fig. 2a dominate the cross section, whereas for $\theta_{c.m.} \sim 180^\circ$

the two diagrams shown in Fig. 2b dominate. Although we are primarily interested in the angular range $\theta_{c.m.} \neq 0, 180^{\circ}$, we found that a very compact formula (yet numerically quite accurate) can be obtained in the following way:

1. By considering the two diagrams in Fig. 2a, the integration can be done exactly. After expanding the result in terms of a double power series in $(p_2 \cdot k)/(p_1 + p_2 - k)^2$ and $m^2/(p_1 + p_2 - k)^2$, and keeping only the lowest power terms, the result can be written as[6]

$$\left(\frac{d\sigma_c}{d\Omega d\omega}\right)_{c.m.} = \frac{\alpha r_o^2 \omega_{c.m.} m^2}{4\pi} \left[\left\{ \frac{4 - 4y + 2y^2}{u^2} - \frac{4m^2 y(1-y)}{u^3} + \frac{2m^4 y^2 (1-y)}{u^4} \right\} \right.$$

$$\left. \times 2\ell n \left[4\gamma_{c.m.}^2 (y^{-1} - 1) \right] - \frac{6 - 6y + 2y^2}{u^2} - \frac{(1-y)}{u^2} \left[\frac{5y^3 m^6}{u^3} - \frac{21 y^2 m^4}{u^2} + \frac{10 y m^2}{u} \right] \right] \tag{9}$$

where $y = \omega_{c.m.}/E_{c.m.}$, $\gamma_{c.m.} = E_{c.m.}/m$, and $u = (p_2 \cdot k)$.
By the nature of its derivation this formula is expected to be correct for $\theta_{c.m.} \ll \frac{\pi}{2}$ and $\omega_{c.m.} \ll E_{c.m.}$. In fact, if we transform this cross section into the laboratory system and make a small angle expansion of $(p_2 \cdot k)$ we obtain exactly the same log terms as those of the Sommerfeld-Schiff formula. The near identity of the small angle $(\theta \ll \gamma^{-\frac{1}{2}})$ energy-angle distribution of bremsstrahlung in the laboratory system for e - e and e - p scatterings is due to the fact that in both cases the minimum momentum transfer to the target can be written as

$$\left| q_{min}^2 \right| \approx \frac{m^4 \omega^2 (1 + \gamma^2 \theta^2)^2}{4E^2 (E - \omega)^2} \ll m^2 \tag{10}$$

Furthermore, $\left| q_{min}^2 \right| \ll m^2$ implies that the target electron receives hardly any recoil at all most of the time, and hence the fact that the target electron is not infinitely heavy is completely inconsequential.

2. We can obtain a similar expression for the cross section valid near $\theta_{c.m.} = 180^\circ$ by considering only the two diagrams shown in Fig. 2b. The result is, of course, identical to the one obtained by making a replacement $p_2 \cdot k \rightarrow p_1 \cdot k$ in Eq. (9).

3. Now we propose that the summation of the two expressions obtained in step 1 and step 2 represents approximately the desired cross section. From the derivation of these two cross sections (small angle expansion, neglect of interference between Fig. 2a and Fig. 2b, and the total neglect of annihilation diagrams) our proposal seems completely unjustified. However, a comparison with the numerical results of S. M. Swanson's exact calculation (column 8 of Table I) shows that the formula thus obtained is correct to within 20% even at $\theta_{c.m.} \approx 90^\circ$ and the error is less than 15% for $\theta_{c.m.} \approx 60^\circ$. By symmetrizing Eq. (9) and tranforming the result into the laboratory system we obtain the following simple expression which is valid for $\gamma\theta \gg 1$:

$$\left(\frac{d\sigma_c}{d\Omega d\omega}\right)_{lab} = \frac{2\alpha r_o^2 \gamma^2}{\pi\omega}\left(\frac{1}{\gamma^4\theta^4} + \frac{1}{4\gamma^2}\right)\left\{2(2 - 2y + y^2)\ln 2\gamma(y^{-1} - 1) - 3 + 3y - y^2\right\}$$

where $y = \omega/\omega_{max}$, and $\omega_{max} = E/\left(1 + \frac{\gamma\theta^2}{2}\right)$. The numerical result of this expression is shown in column 7 of Table I. Column 8 of Table I was obtained by S. M. Swanson, using his computer program for taking traces of γ matrices. The analytical expression for the exact matrix elements (all 8 diagrams) squared contains over 800 terms after cancellations. The computer generated this expression in less than a minute. (It probably took Votruba[8] and Hodes[8] more than a year to obtain similar expressions!!!) The numerical integration with respect to the final e^+e^- was then carried out using this exact expression. Due to the singular nature of the integrand there are some round-off

errors in the numerical result, especially at small ω and small θ. The round-off error is estimated to be less than 5%.

We have not investigated in detail the process (b) except for its effect in the neighborhood of the spike in Fig. 1. An expanded version of Table I from $E = 0.5$ BeV upward will be constructed by Dr. Andrew Dufner at SLAC. We hope the experimenters will be able to use these tables to obtain an optimum angle θ and to estimate the number of background tracks due to Compton electrons and electron pairs in the bubble chamber. If the scheme proves to be feasible, then our tables can be used to estimate the incident flux of the photons for various photoproduction experiments.

The authors wish to thank Sam Howry and Charles Moore of SLAC's Computation Group for carrying out all numerical work for this paper.

LIST OF REFERENCES

1. J. Ballam and Z.G.T. Guiragossián, Proceedings of International Conference on High-Energy Physics, Dubna, 1964 (unpublished).
2. Y. S. Tsai, Phys. Rev. 137, B730 (1965). Numerical examples for δ given here have some arithmetic errors. The author wishes to thank Dr. G. Chadwick for pointing these out to him. The corrections are given in the table following Eq. (7) of this paper.
3. A. Sommerfeld, Wellenmechanik (Unger, New York), p. 551.
4. L. I. Schiff, Phys. Rev. 83, 252 (1951).
5. Y. S. Tsai, Proceedings of International Conference on Nucleon Structure at Stanford (Stanford Press, 1963), edited by R. Hofstadter and L. I. Schiff; p. 225, Eq. (12). Integration with respect to φ_k was done analytically.
6. Y. S. Tsai, unpublished. This formula was originally obtained at the request of Stanford's e^-e^- colliding beam people, and was used for estimating the beam intensity and overlap of two colliding beams. For small angles, the energy-angle distributions are identical for e^+e^- and e^-e^- collisions.
7. S. M. Swanson, "FTRACE: A FAP Subroutine for Dirac Gamma Matrix Algebra," Institute of Theoretical Physics, Stanford University (unpublished). Copies are available upon request.
8. V. Votruba, Bull. Int. Acad. Tcheque des Sciences 49, 19 (1948) and Phys. Rev. 73, 1468 (1948).

   I. Hodes, Ph.D. thesis, University of Chicago (1953), unpublished.

LIST OF FIGURES

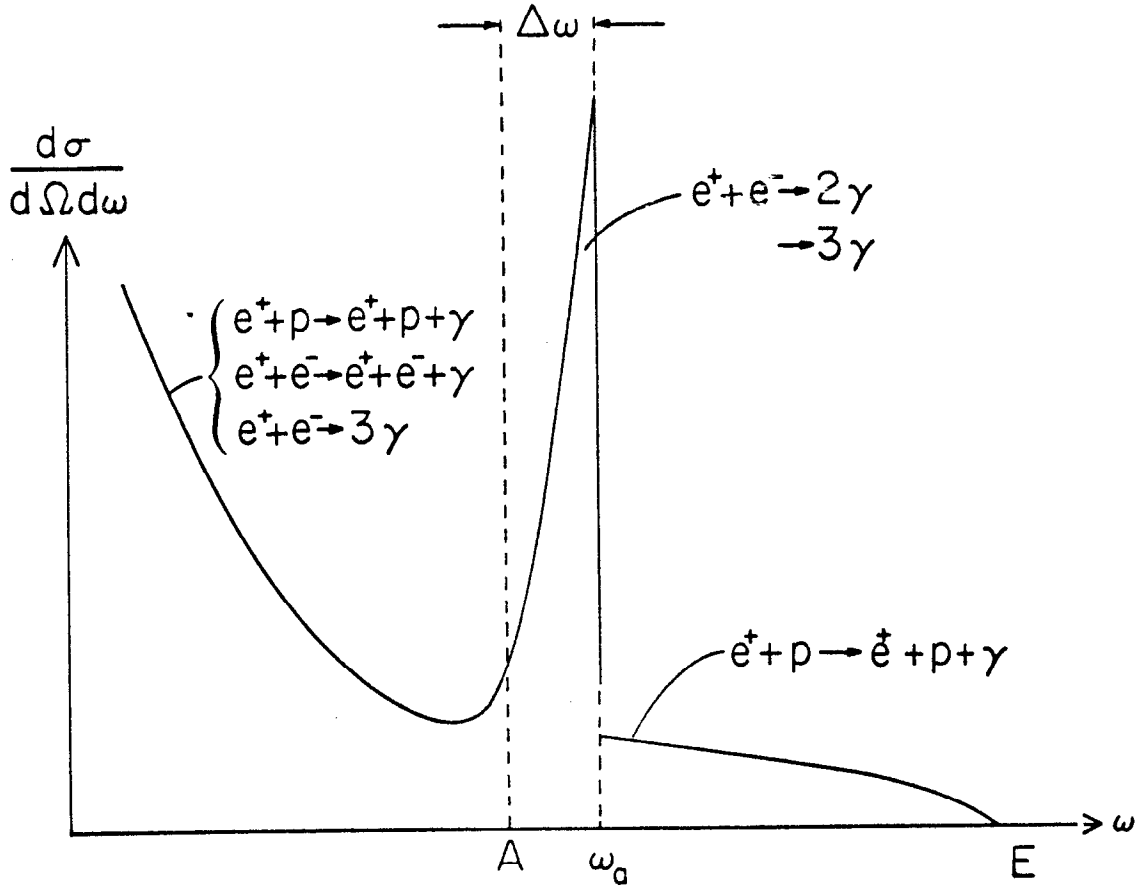

309-1-A

FIG. 1 -- A TYPICAL GAMMA SPECTRUM OF POSITRON-HYDROGEN ATOM COLLISION AT A FIXED ANGLE.

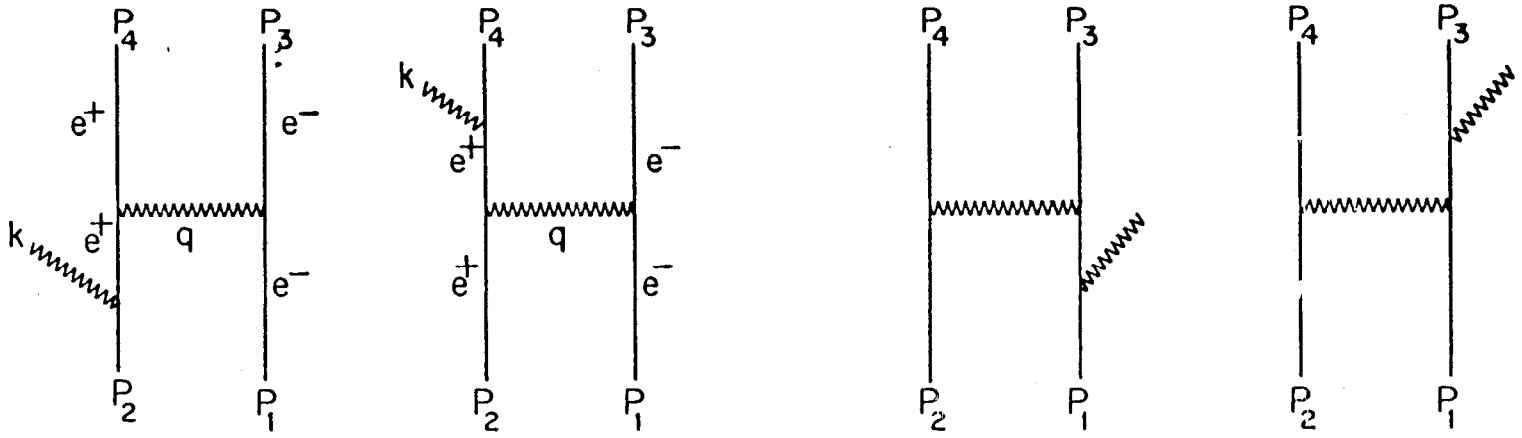

(a)

(b)

FIG 2 --(a) THE TWO DIAGRAMS WHICH DOMINATE SMALL ANGLE ($\theta_{CM} \sim 0$) BREMSSTRAHLUNG IN THE $e^+ e^-$ COLLISION. (b) CORRESPONDING DIAGRAMS WHICH DOMINATE AT $\theta_{CM} \sim 180°$.

309-2-A

TABLE I

E = 15 BeV

θ_{lab}	$\theta_{c.m.}$	ω_{lab}	$e^+ + e^- \rightarrow 2\gamma$	$e^+ + p \rightarrow e^+ + p + \gamma$ Schiff	$e^+ + p \rightarrow e^+ + p + \gamma$ Exact	$e^+ + e^- \rightarrow e^+ + e^- + \gamma$ Tsai	$e^+ + e^- \rightarrow e^+ + e^- + \gamma$ Exact
Rad	Rad	BeV	10^{-25}cm^2/sr	10^{-25}cm^2/sr/BeV	10^{-25}cm^2/sr/BeV	10^{-25}cm^2/sr/BeV	10^{-25}cm^2/sr/BeV
2×10^{-3}	0.475	0.02		630.0	870.3*	900.0	893.0
		0.05		253.0	330.0*	340.0	336.0
		0.1		126.0	160.0*	162.0	160.0
		0.5		24.5	27.9*	28.1	27.7
		1.0		11.8	12.7*	12.8	12.6
		2.0		5.39	5.62*	5.62	5.49
		4.0		2.25	2.27	2.27	2.19
		6.0		1.25	1.27	1.26	1.19
		8.0		0.810	0.814	0.801	0.728
		10.0		0.564	0.563	0.552	0.475
		12.0		0.413	0.411	0.398	0.310
		14.0		0.298	0.296	0.232	0.199
		14.170	6.05			0.0	0.0
5×10^{-3}	1.089	0.02		18.7	22.8*	25.7	22.7
		0.05		7.47	8.60*	9.67	8.50
		0.1		3.71	4.09*	4.60	4.01
		0.5		0.7	0.710*	0.788	0.676
		1.0		0.322	0.325*	0.356	0.302
		2.0		0.142	0.143	0.152	0.127
		4.0		0.0580	0.0580	0.0590	0.0475
		6.0		0.0324	0.0323	0.0316	0.0242
		8.0		0.0208	0.0206	0.0195	0.0142
		10.0		0.0144	0.0142	0.0127	0.00955
		10.97	0.657			0.0	0.0
		12.0		0.0106*	0.0104	0.0	0.0
		14.0		0.00764*	0.00746	0.0	0.0
8×10^{-3}	1.54	0.02		3.05	3.42*	6.35	5.51
		0.05		1.21	1.29*	2.39	2.05
		0.1		0.599	0.613*	1.13	0.965
		0.5		0.108	0.106	0.190	0.159
		1.0		0.0493	0.0485	0.0840	0.0693
		2.0		0.0217	0.0211	0.0344	0.0279
		4.0		0.00885	0.00869	0.0123	0.00964
		6.0		0.00495	0.00483	0.00629	0.00480
		7.734	0.212			0.0	0.0
		8.0		0.00317	0.00308	0.0	0.0
		10.0		0.00220*	0.00213	0.0	0.0
		12.0		0.00161*	0.00154	0.0	0.0
		14.0		0.00117*	0.00110	0.0	0.0
12×10^{-3}	1.94	0.02		0.635	0.662*	3.53	3.08
		0.05		0.250	0.249	1.32	1.14
		0.1		0.122	0.119	0.622	0.534
		0.5		0.0213*	0.0205	0.101	0.0843
		1.0		0.00975*	0.00933	0.0425	0.0350
		2.0		0.00428*	0.00408	0.0161	0.0127
		4.0		0.00175*	0.00165	0.00511	0.00377
		4.82	0.106			0.0	0.0
		6.0		0.000978*	0.000917	0.0	0.0
		8.0		0.000626*	0.000582	0.0	0.0
		10.0		0.000435*	0.000401	0.0	0.0
		12.0		0.000319*	0.000290	0.0	0.0
		14.0		0.000230*	0.000205	0.0	0.0